Derivation of aerosol properties from polarized observations

Didier Tanré,

CNRS/Université de Lille

Most of the French studies were supported by cnes

4-7 November 2019, Lille, France.

Aerosol properties derived from polarized observations

- The number of polarimetric observations is increasing.
- Why polarization is attractive?
- What type of informations can be derived?
- Incomplete (and biased!) summary.

Aerosol properties derived from polarized observations: Venus

- In the 50's polarization observations were made for planets like Jupiter, Mars, Saturn, Mercury and mainly Venus because of its dense atmosphere (e.g. Coffeen, Dollfus, Gehrels, etc)

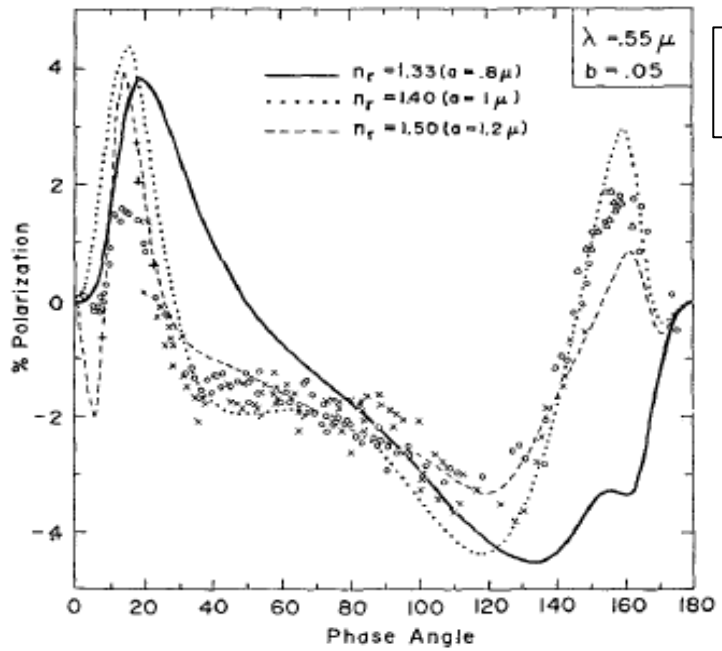

FIG. 6. Observations are the same as in Fig. 4. The theoretical curves are for three refractive indices with the effective particle radius chosen in each case to yield the best agreement with the observations. The size distribution is (8) with $b=0.05$. The Rayleigh contribution to the phase matrix is given by $f_R=0.045$

Cloud particles size follows a Gamma Distribution

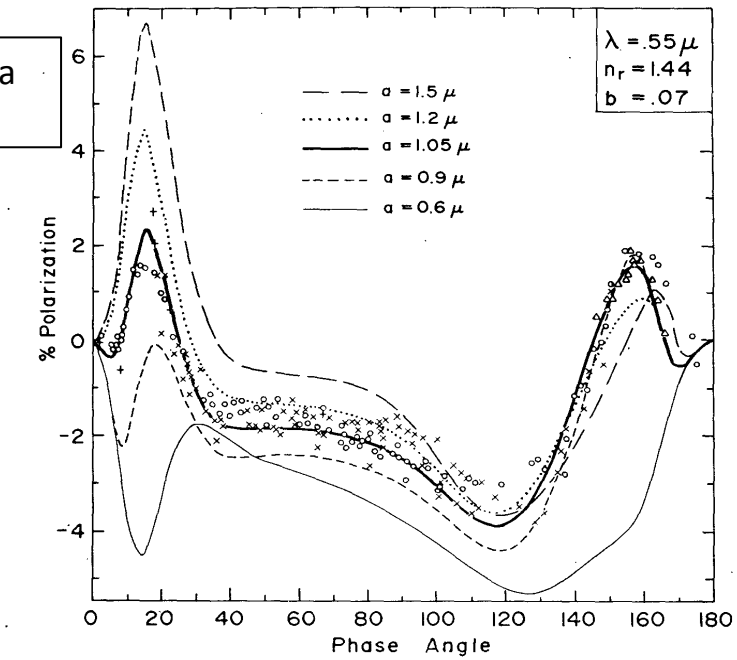

FIG. 4. Observations of the polarization of sunlight reflected by Venus in the visual wavelength region and theoretical computations for $\lambda=0.55$ μm. The ○'s are wide-band visual observations by Lyot (1929) while the other observations are for an intermediate bandwidth filter centered at $\lambda=0.55$ μm; the ×'s were obtained by Coffeen and Gehrels (1969), the +'s by Coffeen (cf. Dollfus and Coffeen, 1970), and the Δ's (which refer to the central part of the crescent) by Veverka (1971). The theoretical curves are all for a refractive index 1.44, the size distribution (8) with $b=0.07$, and a Rayleigh contribution $f_R=0.045$. The different curves show the influence of the effective radius on the polarization.

Analysis of VENUS ground-based polarimetry (from Hansen and Hovenier, JAS, 1974)

Aerosol properties derived from polarized observations: Venus

- Polarized observations by the Orbiter Cloud Photo Polarimeter (OCPP) in 1978 (Pioneer Venus Mission, Travis et al., 1979)

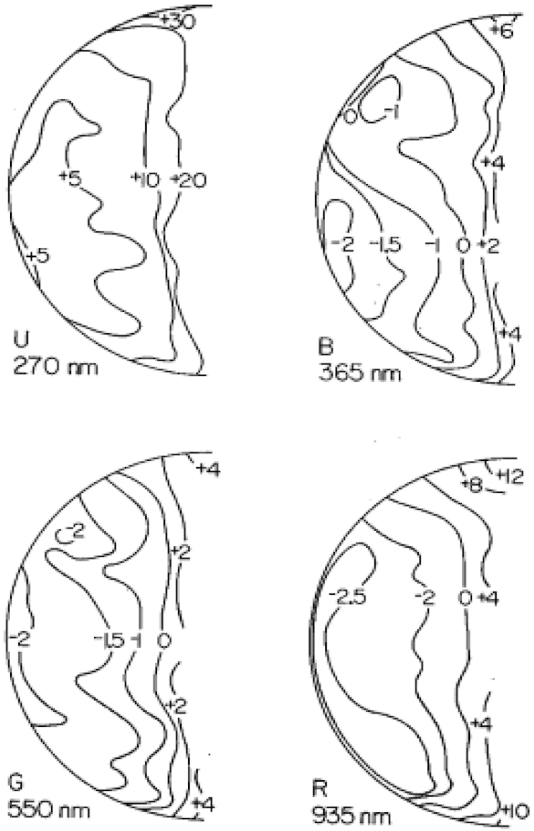

Fig. 4. Contour maps of linear polarization at the four OCPP polarimetry wavelengths. The observations were made on 13 December 1978, when the phase angle was 96° (*15*). The center of the visible disk is at 13°N latitude, with north at the top. The instantaneous field of view is approximately 280 km at the subspacecraft point. The positive polarization at 270 nm is produced by Rayleigh scattering from gas in and above the visible clouds. The negative polarization at the longer wavelengths is caused by sulfuric acid particles of 1 μm radius, while the positive values at the poles and terminator in the 935 nm map require the existence of a thin haze layer of small particles above the main cloud.

- Existence of a haze layer above the clouds (same refractive index m=1.44) particles with radius not larger than 0.4 µm and optical thickness of 0.05 to 0.1 in the visible

Aerosol properties derived from polarized observations

- These are typical examples but there are other studies available for Mars (dust storms) or Venus (VENERA/USSR, MARINER/USA)

- Needs for advanced « tools »:
  - Full scattering properties using Mie theory
  - Development of Polarized Radiative Transfer models for exploiting such polarimetric observations

See the pioneer works of Van de Hulst, Chandrasekhar, Hansen, Hovenier, Coffeen, Kattawar, Sobolev, Sekera, Deirmendjian, Lenoble, Herman, etc).

Aerosol properties derived from polarized observations of the earth in the solar spectrum

- Polarized transmitted radiances
  - Ground-based observations
  - Stratospheric balloons (stratosphere)

- Polarized reflected radiances
  - Airborne imaging polarimeters sensors (POLDER, RSP, AirMSPI, SPEX, AirHARP, Airborne DPC, etc;
  - Satellite sensors.

Aerosol properties derived from Ground-based polarized observations

- First observations Arago in 1809, (Coulson, Sekera, etc)

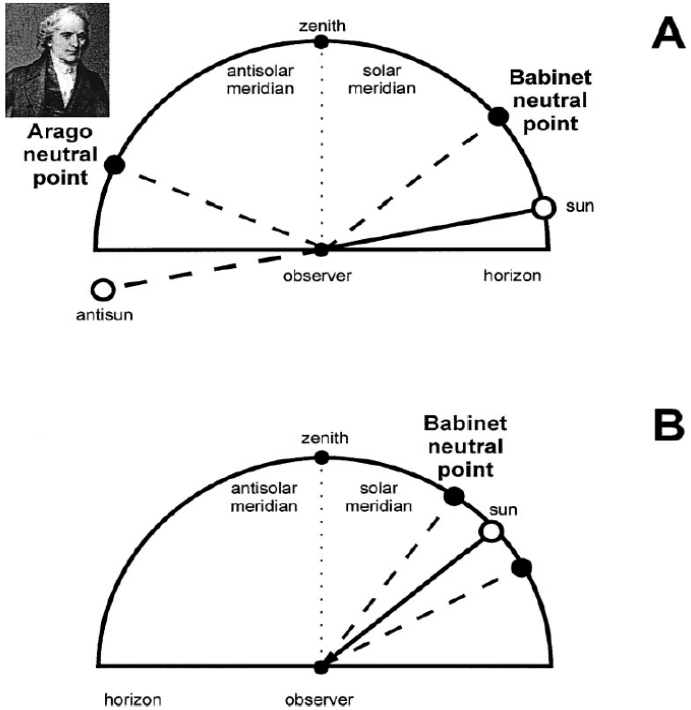

Fig. 1A,B. Schematic diagram showing the normal positions of the Arago, Babinet, and Brewster neutral points of skylight polarization in the plane of the sun's vertical. *Insets*, the portraits of Dominique Francois Jean Arago (1786–1853) and Sir David Brewster (1781–1868), the discoverer of the first and third neutral points, respectively

Illustration from Horváth et al., 1998

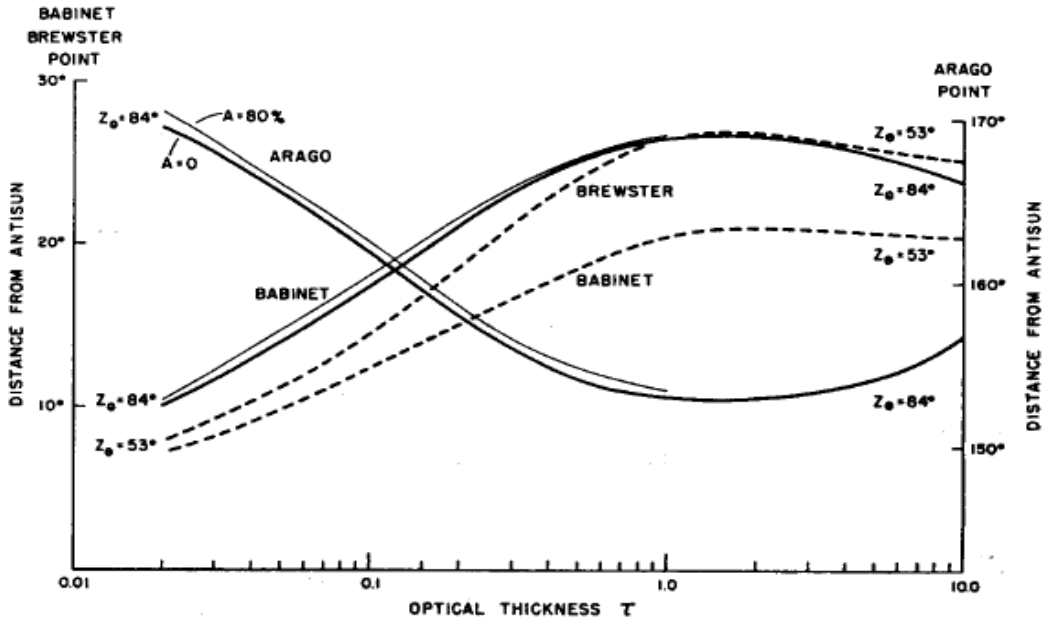

FIG. 1. Positions of neutral points of the radiation emerging from the top of a Rayleigh atmosphere.

From Sekera, 1967 and based on computations made by Dr. J. V. Dave,

Aerosol properties derived from Ground-based polarized observations: AERONETsun-photometers

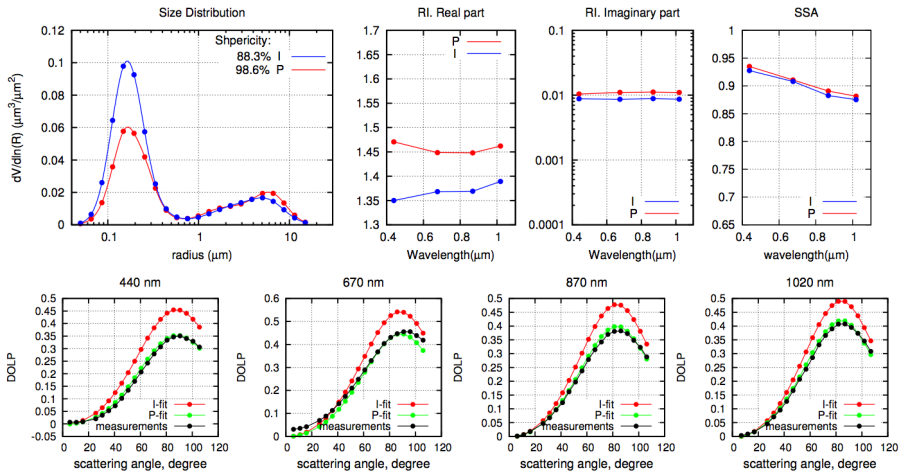

FIGURE B.5: Size Distribution, Refractive Index and Single Scattering Albedo. 29/07/2011, GSFC, $\theta_s = 32.2°$, $\tau_{440} = 0.58$

Urban site (GSFC)

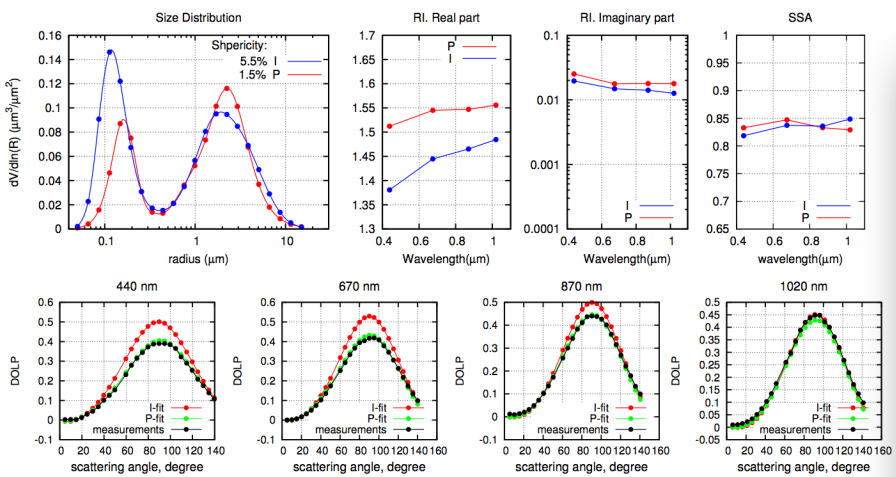

FIGURE B.15: Size Distribution, Refractive Index and Single Scattering Albedo. 11/01/2013, Dakar, $\theta_s = 66.7°$, $\tau_{440} = 0.91$

Desert dust (Dakar)

- « Extreme » cases.
- Use of polarization brings information for the fine mode dominated aerosols
- High sensitivity of polarimetric data to particle shape and models for non-spherical particles are needed (see works of Bohren Dubovik, Mischenko, Muñoz, Volten,…)
- Real part of the refractive index (no effect on SSA)

More results : Sinyuk et al., Monday **17:00– 17:15**

Li et al., JQSRT, 2009
Fedarenka et al.. JQSRT, 2016

Stratospheric Aerosol properties derived from ballon polarized observations

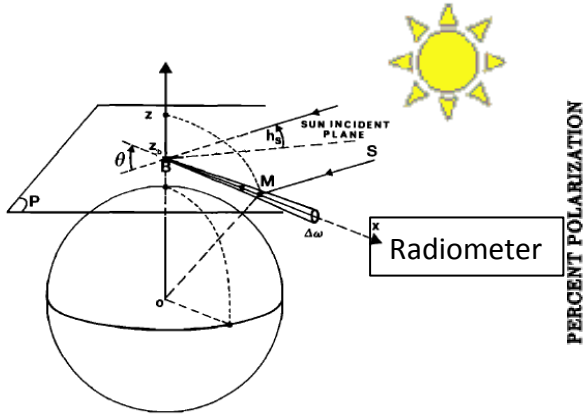

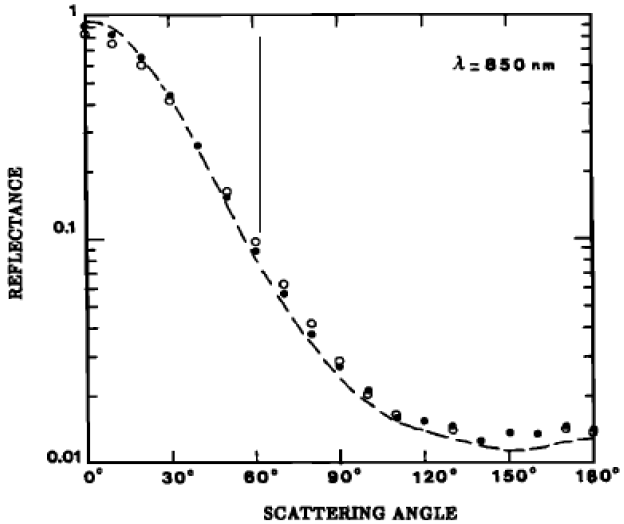

Fig. 21. Same as Figure 18, but for the reflectances at $\lambda = 850$ nm. The good agreement here confirms the nominal calibration.

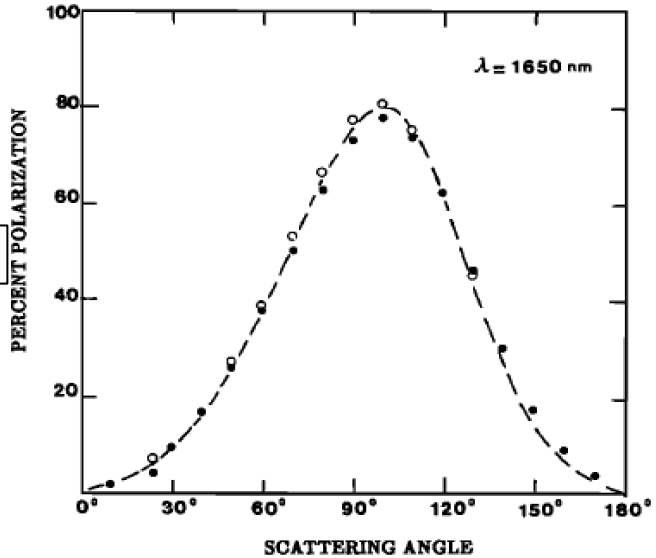

Fig. 18. Polarization ratios as a function of the scattering angle θ, at $\lambda = 1650$ nm. The measurements performed for $h_s = 0°$ have been smoothed by the continuous curve. The circles are the results of the Monte Carlo code for the lognormal aerosol model, adjusted by matching, from single scattering calculations, the corrected measurements $P_{1650}^*(100°)$ and $P_{850}^*(100°)$. The dots are the same results, but for the gamma modified aerosol model, selected by matching the whole corrected diagrams $P_{1650}^*(\theta)$ and $P_{850}^*(\theta)$..

(hydrated sulfuric acid particles m=1.45)

Herman et al., AO, 1986
Santer et al., JGR, 1988

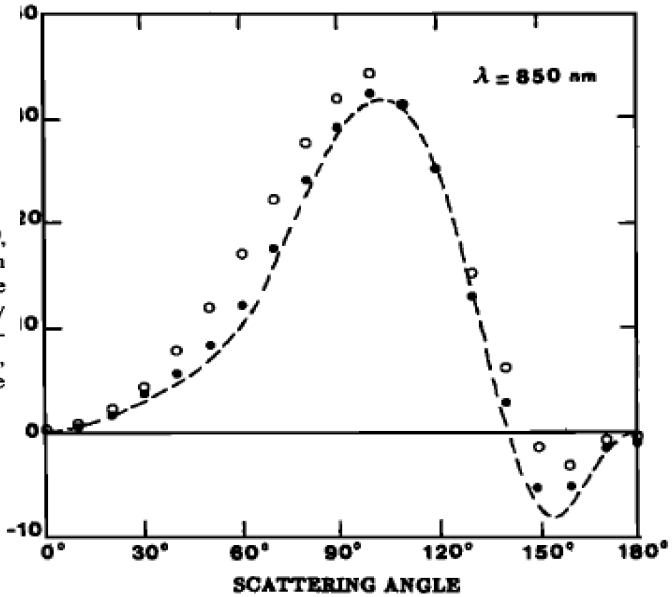

Fig. 20. Same as Figure 18, but for the polarization ratios at $\lambda = 850$ nm. The gamma-modified model greatly improves the fit.

Radiative Transfer considering spherical geometry (Monte Carlo)

Aerosol properties derived from reflected polarized observations

- The major Challenge is the surface or underlying layer contribution.

- Airborne imaging polarimeters sensors (usually simulators for space instruments, see papers by Chowdhary, Cairns, Deuzé, Diner, Vanderlei, Knobelspiesse, Gu, Cheng, etc)

- Satellite sensors:
  - First multiangle satellite instrument measuring polarization in the solar domain is (POLDER-1) lauched in 1996 on the ADEOS-1 platform (with 8 months of data), followed by POLDER-2 on ADEOS2 in 2002 (with 7 months of data) and by POLDER-3 on PARASOL in 2004 (with 8.5 years of data and 5 years within the A-Train)
  - For more than 20 years, the POLDER's serie remained the only instrument that measures the polarization of the Earth reflectances (Polarization capabilities of GOME, GOME2 and SCIAMACHY, were too limited to use for aerosol retrieval).
  - Recently: SGLI (limited polarimetric capabilities: 2 directions/2 wavelenghts 670/865) was launched in December 2017 on GCOM-C1 *(see presentation by I. Sano Wednesday 9:00 – 9:20)* and the Directional Polarimetric Camera (DPC) (similar to POLDER) launched in May 2018 on GF-5 satellite MAI/TG-*2 (see presentation by Z. Li Monday 14:40 – 14:55)*.

(Calibration, registration, etc, see papers by B. Fougnie et al., IEEE, 2009, 2016)

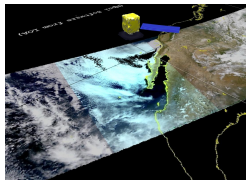

Aerosol properties derived from satellite polarized observations over ocean

Easier over Ocean thanks to Cox and Munk model (JOSA) published in 1954!!.

$$R = \frac{\bar{L}_a(670nm)}{\bar{L}_a(865nm)}$$

Fine Spherical mode
Coarse mode : mixture of spheres and spheroids

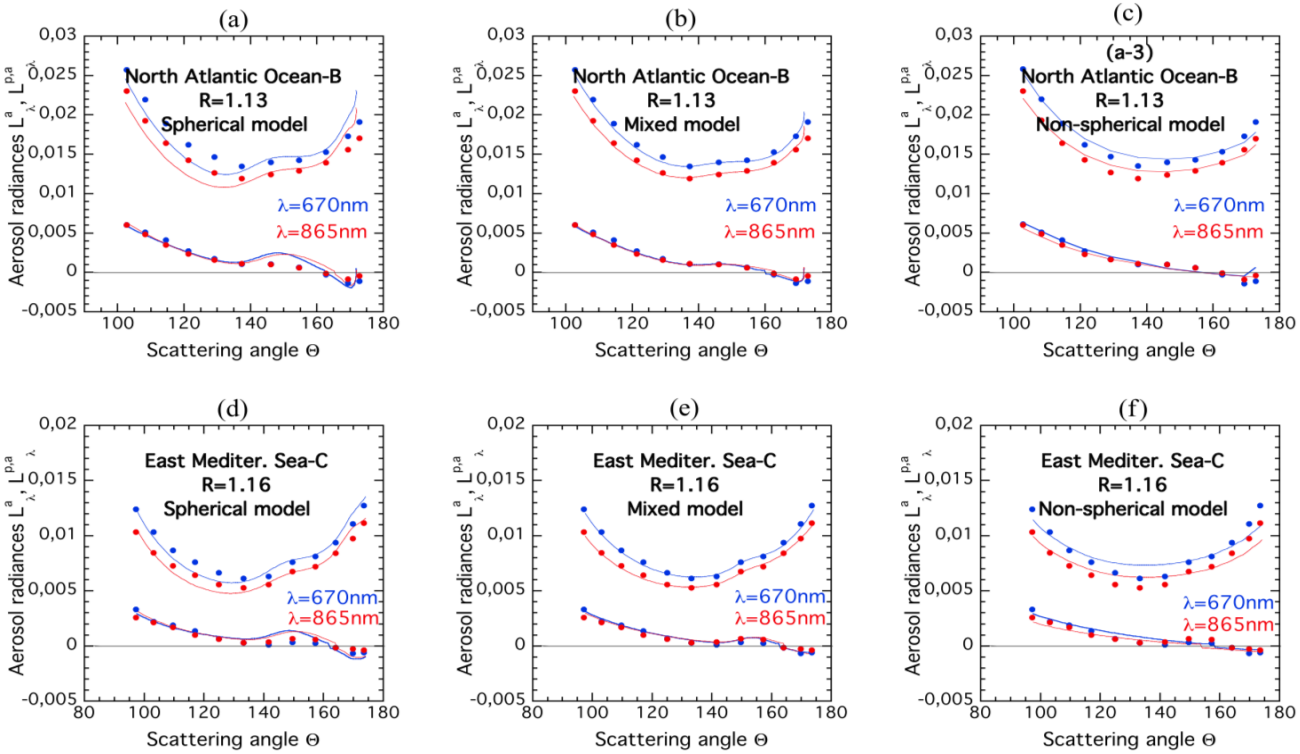

Figure 8. Same as Figure 3 (dots, measurements; continuous curves, best fit). (a and d) Best fit with coarse modes of spherical particles. (c and f) best fit with the nonspherical model of *Volten et al.* [2001] for the coarse mode. (b and e) Best fit with coarse modes mixing spherical and nonspherical particles.

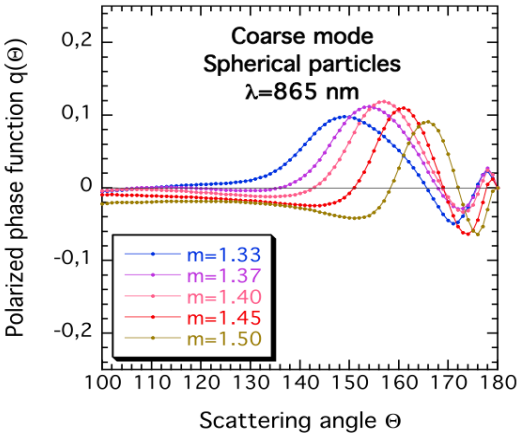

Figure 10. Polarized phase function, $q_\lambda(\Theta)$, of a typical coarse mode of spherical particles ($\bar{r} = 0.75$ µm, $\sigma = 0.70$) as a function of Θ, for different values of the refractive index, m_c, $\lambda = 865$ nm. The localization of the polarized rainbow maximum around $\Theta = 150°$ excludes values of m_c larger than about 1.40. The sensitivity of $q_\lambda(\Theta)$ to the particle radius, $\bar{r}$, of the coarse mode is much less and is not illustrated.

Deuze et al., JGR, 2000,
Herman et al., JGR, 2004
Hasekamp et al, 2011

Aerosol properties derived from satellite polarized observations over Land

- Surface polarized reflectance (BPDF):
  - over vegetated areas: small and pretty uniform and can be parametrized as a function of surface type and NDVI (semi empirical model ; review Breon and Maignan, Earth Syst. Sci. Data, 9, 31–45, 2017.
  - desert or snow: larger polarized reflectance, more challenging

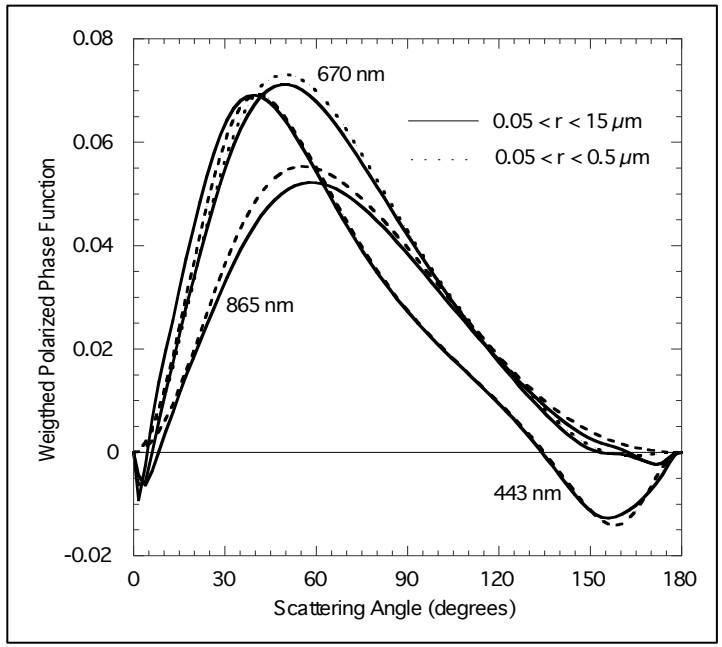

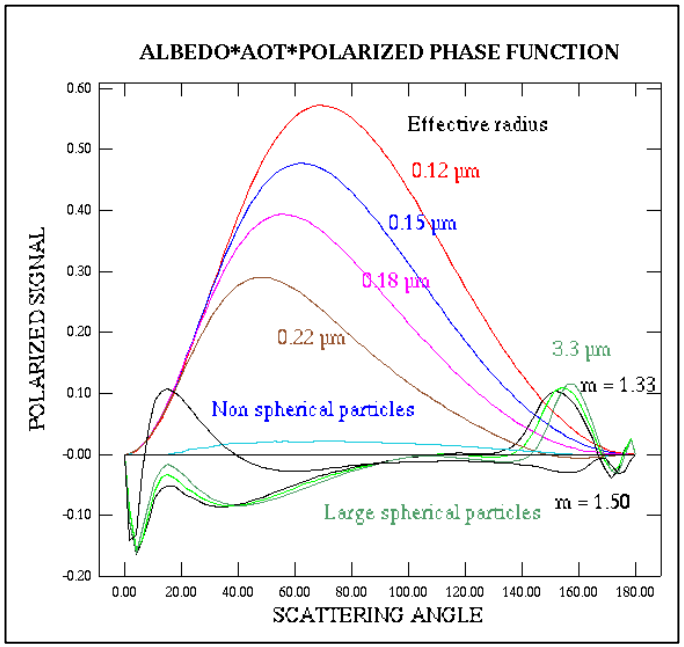

- Algorithm is based on polarized reflectances at 670 and 865 nm.
  - Fine mode (sulfates, biomass burning) + optical thickness
  - Does not work for coarse non-spherical aerosols (desert dust)

Herman et al., JGR, 1997
Deuze et al., JGR, 2001,

Aerosol properties derived from satellite polarized observations over Land: new approach

Dubovik et al., 2011, 2014

- Development of statistically optimized inversion algorithm.

- GRASP (Generalized Retrieval of Aerosol and Surface Properties): Retrieval use practically no information about surface and type of aerosol and both bi-directional intensity & polarization reflectance and aerosols are retrieved simultaneously

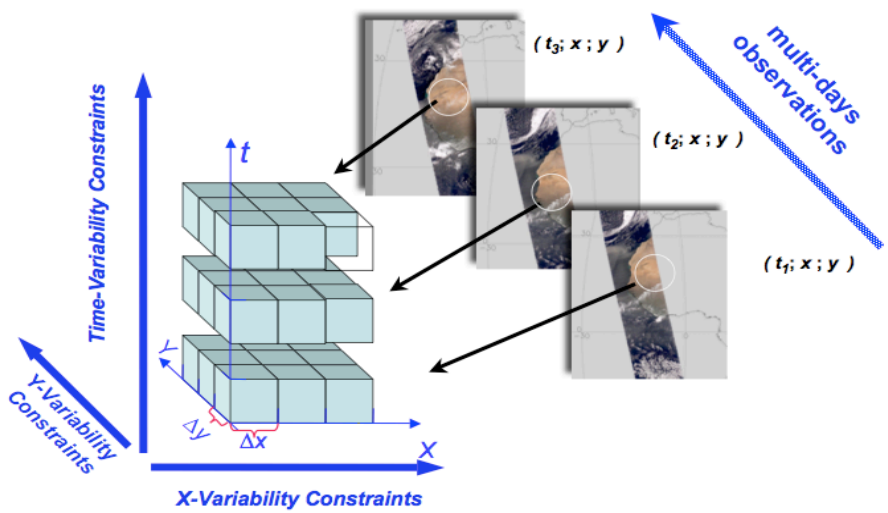

- Concept of multi-pixel retrieval
- Detailed aerosol informations (size distribution, absorption, chemical composition, aerosol height)

(see presentation by O. Dubovik Tuesday 10:00 – 10:15)

Aerosol properties derived from satellite polarized observations over clouds

Waquet et al., JAS, 2009, AMT, 2013, JGR, 2016

Peers et al., ACP, 2015

the scattering AOT is set

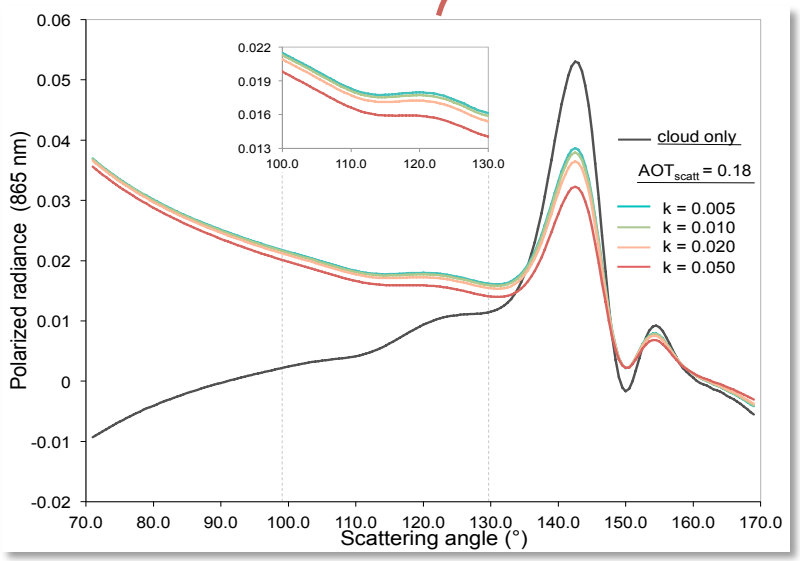

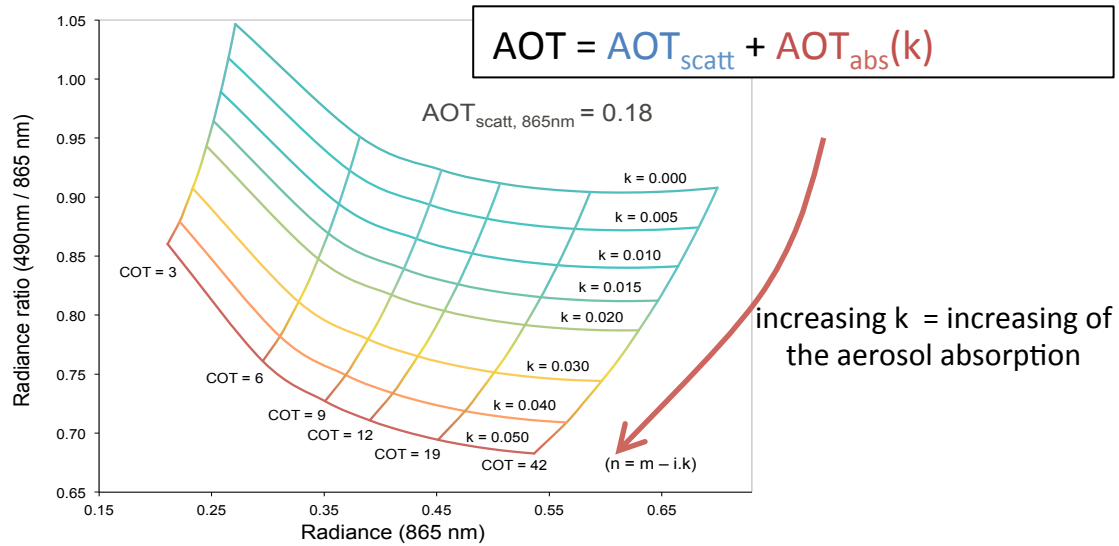

- Polarized radiances are mostly sensitive to scattering processes.
- Cloud + fine mode aerosol *(r_{eff} = 0.1µm)*: Additional polarization at side scattering angle

Radiances at 490 and 865 nm can be interpreted as a coupled COT and absorption AOT since the scattering optical thickness of aerosol and their size are known.

(see presentation by F. Waquet Tuesday 11:00 – 11:15)

CONCLUSION

- With new generation retrieval algorithms exploiting multidirectional polarimetric observations :
  - Almost no restriction to prescribed aerosol models and retrieval of AOD, size distribution, refractive index, altitude.
  - Simultaneous retrieval of surface properties, retrievals are possible over all types of land surfaces and also above clouds.

- SWIR (1.6 and 2.2µm) additional information will improve the retrieval of coarse mode aerosols

- Extension of spectral range toward shorter wavelength will improve the aerosol speciation through the spectral SSA (and retrieval of layer altitude)

- Aerosols and clouds interactions:
  - high resolution is needed.
  - Radiative transfer models taking into account 3D effects (such as shadows, cloud induced enhancements, etc) are needed (Stap et al., 2016; Emde et al., 2018).
  - Needs for core-shell particle models (aerosol in-cloud processes).

Future Missions

- Extensive review of future polarized missions in Dubovik et al., JQSRT, 2019.

- Two missions that will be launched soon :
  - Fougnie et al., JQSRT, 2019 (3MI)
  - Remer et al., Front. Earth Sci., 2019 (PACE)

- Projects presented during the conference:
  - T. Marbach, 3MI, Monday 11:50 – 12:10
  - D. Diner, MAIA, Monday 14:20 – 14:40
  - A. AlMaazmi, DMSAT-1, Monday 15:10– 15:25
  - B. Cairns, PACE, Tuesday 11:30-11:50
  - J. Vanderlei Martins, HARP, Tuesday 11:50 – 12:10
  - O. Hasekamp, SPEXone, Tuesday 12:10 – 12:30
  - G. Milinevsky, Aerosol-UA, Wednesday, 9:20 – 9:40

+ Airborne simulator measurements during field experiments